JBC Papers in Press. Published on October 12, 2010 as Manuscript M110.163535
The latest version is at http://www.jbc.org/cgi/doi/10.1074/jbc.M110.163535

Characterization of a hemophore-like protein from *Porphyromonas gingivalis*

Jin-Long Gao[1, 2], Ky-Anh Nguyen[1, 2], Neil Hunter[1]
From the [1]Institute of Dental Research, Westmead Millennium Institute and Centre for Oral Health, Westmead Hospital, Sydney, NSW, Australia and the
[2]Faculty of Dentistry, The University of Sydney, NSW, Australia
Running title: HusA hemophore in *P. gingivalis*
Address correspondence to: Ky-Anh Nguyen, BDS, PhD. PO Box 533, Wentworthville NSW 2145 Australia. Tel: +61 2 9845 8766; Fax: +61 2 9845 7599. Email: kyanhn@gmail.com

The porphyrin auxotrophic pathogen *Porphyromonas gingivalis* obtains the majority of essential iron and porphyrin from host hemoproteins. To achieve this, the organism expresses outer membrane gingipains containing cysteine proteinase domains linked to hemagglutinin domains. Heme mobilised in this way is taken up by *P. gingivalis* through a variety of potential portals where HmuY/HmuR of the *hmu* locus are best described. These receptors have relatively low binding affinities for heme. In this report, we describe a novel *P. gingivalis* protein, HusA, the product of *PG2227*, which rapidly bound heme with a high binding constant at equilibrium of 7 x 10^{-10} M. HusA is both expressed on the outer membrane and released from the organism. Spectral analysis indicated an unusual pattern of binding where heme was ligated preferentially as a dimer. Further, the presence of dimeric heme induced protein dimer formation. Deletional inactivation of *husA* showed that expression of this moiety was essential for growth of *P. gingivalis* under conditions of heme limitation. This finding was in accord with the pronounced increase in gene expression levels for *husA* with progressive reduction of heme supplementation. Antibodies reactive against HusA were detected in patients with chronic periodontitis, suggesting that the protein is expressed during the course of infection by *P. gingivalis*. It is predicted that HusA efficiently sequesters heme from gingipains and fulfils the function of a high affinity hemophore-like protein to meet the heme requirement for growth of *P. gingivalis* during establishment of infection.

Microorganisms rely on iron for a wide range of metabolic and signaling functions. A significant amount of iron in the host is co-ordinately bound to heme (Fe^{2+}PPIX) or hemin (Fe^{3+}PPIX), a prosthetic group of many biologically active proteins such as hemoglobin, myoglobin and cytochromes. Although formal definitions distinguish "heme" and "hemin", the term "heme" is widely used to indicate iron protoporphyrin IX in any oxidation state. As a major biological iron source for microbes, heme is also an important porphyrin source for certain bacterial species such as *Hemophilus influenzae* and *Porphyromonas gingivalis* that are unable to synthesize the tetrapyrrole ring *de novo* (1-2). Bacteria have developed two general systems to scavenge heme from their environs. The first involves synthesis of specific outer membrane receptors enabling direct contact between the organism and exogenous heme sources; for instance, HmuR, an outer membrane protein with relatively low heme binding affinity in *P. gingivalis* (3). The second strategy depends on secretion of heme capturing molecules, hemophores, which scavenge free heme or heme from various carriers. There are currently only three characterized hemophores in the bacterial kingdom: two in Gram-negative bacteria including HasA in *Serratia marcescens* (4) and HxuA in *Hemophilus influenzae* (5) and one in a Gram-positive organism being the IsdX1 in *Bacillus anthracis* (6).

Porphyromonas gingivalis, a Gram-negative anaerobe, is a leading pathogen in chronic periodontitis, a disease process involving progressive destruction of teeth-supporting tissues, including bone (7). There is also convincing data from experimental models and clinical investigations revealing that *P. gingivalis* contributes to atheromatous plaque formation that predisposes to heart disease and stroke (8). Within the periodontopathic microbiota involved in periodontal disease, *P. gingivalis* is reported as one of the early colonizers of dental plaque with other bacterial species in the development of

dental plaque biofilms (9-10). For successful colonisation of the gingival crevice, *P. gingivalis* must acquire heme from limited quantities of host hemoproteins in the healthy gingival crevice, as well as compete with other heme/iron requiring microorganisms to scavenge essential heme (11). Due to the absolute requirement of heme for growth of this organism, it has been speculated that *P. gingivalis* may utilise a hemophore as a heme scavenger although no candidate has been detected.

Here, we report the characterization of the product of *PG2227* as a novel hemophore-like heme binding protein HusA (heme uptake system protein A) detected in *P. gingivalis* growing under continuous culture in heme-limited conditions. HusA was found to be a high-affinity heme binding protein which preferably binds the ligand as μ-oxo dimeric heme. Further, our finding indicates that *P. gingivalis* responds to heme limitation by producing HusA as an outer membrane-associated protein as well as releasing it into the culture medium to act as a heme scavenger.

Experimental Procedures

Bacterial strains and growth conditions. *Porphyromonas gingivalis* wild-type strain W83 and mutant derivatives were grown in enriched tryptic-soy broth (eTSB; per liter: 30 g Trypticase soy broth, 5 g yeast extract, 5 mg hemin, pH 7.5, supplemented with 5 mM L-cysteine and 2 mg menadione) or blood eTSB agar (eTSB medium plus 15 g/L agar and supplemented with 3% defibrinated sheep blood) at 37°C in an anaerobic chamber (Don Whitley Scientific Limited, U.K.) with an atmosphere of 90% N_2, 5% CO_2, and 5% H_2. *Escherichia coli* strain DH5α was used for all plasmid construction work and was grown in Luria-Bertani broth medium and agar. For antibiotic selection in *E. coli*, ampicillin was used at 100 μg/ml and erythromycin used at 300 μg/ml. For *P. gingivalis* growth selection on solid media, erythromycin was used at 5 μg/ml and doubled in liquid culture. The phenotype and genotype of all strains and plasmids are listed in Table S1.

For continuous culture, *P. gingivalis* W83 was grown in a custom-designed chemostat system with a 70 ml working volume. Overnight *P. gingivalis* start culture was inoculated at 1:25 into modified basal medium (BM; per liter: 10 g proteose peptone, 5 g yeast extract, 5 g tryptone, 2.5 g KCl, 5 mM L-cysteine and 2 mg menadione, pH 7.5) supplemented with hemin at various concentrations. The dilution rate was 0.05 h^{-1}, giving a mean generation time of 13.9 h; the pH was maintained at 7.5 ± 0.1. Once steady state growth was established, cultures were harvested at 4°C. The biomass of the culture was monitored by optical density (Beckman DU640, Beckman Coulter, USA), and culture purity was checked by Gram-staining.

Production and purification of recombinant HusA. The *husA* gene was amplified by PCR from *P. gingivalis* W83 genomic DNA using rPG2227NcoIF, rPG2227XhoIR primers (see Table S2) and Accuprime Pfx DNA polymerase (Invitrogen, USA) and subsequently cloned into NcoI and XhoI sites of the T7 expression pET24d(+) plasmid (Novagen, Merck Group, Germany) to create the plasmid pETR7. The final gene construction encodes for HusA minus the first 23 amino acid residues of a putative signal peptide sequence as predicted by SignalP 3.0 (*http://www.cbs.dtu.dk/services/SignalP/*). The stop codon of *husA* was replaced by a thrombin cleavage site followed by a C-terminal 6×histidine tag.

E. coli strain BL21 (DE3) (Invitrogen, USA) carrying the plasmid pETR7 was grown in 50 ml of LB medium with 50 μg/ml kanamycin at 37°C overnight before being inoculated into 1L pre-warmed LB/kanamycin medium with vigorous shaking at 37°C. At OD_{600} 0.6, 0.5 mM isopropyl-*ß*-D-thiogalactopyranoside (IPTG) was added and the culture was allowed to grow for an additional 3 hours before harvesting. Bacteria were sedimented by centrifugation and resuspended in cold native lysis buffer (50 mM NaH_2PO_4, 300 mM NaCl, and 10 mM imidazole, pH 8.0) at approximately 5 ml/g pellet followed immediately by a freeze-thaw process. Bacteria were lysed by pulse-sonication on ice and the supernatant was passed through a Ni-chelating resin to purify the 6×His tagged protein (Qiagen, Australia). Purified protein was dialyzed into 100 mM Tris, pH 8.0, 250 mM NaCl before the addition of 10 mM $CaCl_2$ for thrombin cleavage. The 6×His tag was removed from the fusion HusA using the Thrombin CleanCleave™ kit (Sigma-Aldrich, Australia) at 4°C according to the manufacturer's instructions. Cleaved 6×His

fragments were removed through a Ni-chelating column and the de-tagged rHusA was dialyzed and concentrated into 100 mM Tris, pH 8.0, 250 mM NaCl.

Heme solutions preparation. All heme solutions were prepared immediately before use. Fresh 10 mM stock solution of hemin (>98% HPLC Fluka, USA) in 0.1 M NaOH was diluted into 100 mM Tris buffer, pH 8.0 for μ-oxo bisheme binding assays. To obtain heme solutions comprising predominantly of monomeric heme, the pH of the 10 mM stock solution was adjusted to pH 7.5 by slow drop-wise addition of HCl followed by dilution into 50 mM PIPES buffer, pH 6.5 (12). Surface heme-containing pigments from *P. gingivalis* colonies on blood agar were extracted by incubation in 140 mM NaCl, 100 mM Tris, pH 9.8, for 10 min at 20°C (13). Heme concentration in the extracted pigment solution was calculated using the heme molar extinction coefficient $\varepsilon_{385} = 58{,}400$ (14)**.**

HusA heme binding assays

a) Tetramethylbenzidine (TMBZ) staining. Heme staining of SDS−PAGE gels by TMBZ/H_2O_2 detects heme bound to proteins. Samples subjected to PAGE were pre-treated with conventional reducing sample buffer, with or without boiling. After electrophoresis, gels were fixed in the dark for 1 hour in a pre-chilled solution of sodium acetate (250 mM, pH 5.0)-methanol-H_2O at a ratio of 6:3:1 (v:v). Gels were stained with 7:2:1 (v:v) of sodium acetate (250 mM, pH 5.0)-TMBZ (6.3 mM in methanol)-H_2O for 30 mins, followed by color development with 30 mM H_2O_2 for 30 mins at 4°C in the dark.

b) Hemin-agarose binding. Briefly, rHusA was mixed and incubated with pre-washed hemin-agarose (Sigma-Aldrich, Australia) in 100 mM NaCl, PBS buffer, pH 7.4 for 3 h at 37°C. Non-specifically adsorbed proteins were washed off with 1 M NaCl, PBS and 0.5% Sarkosyl and bound proteins were eluted with SDS-PAGE sample buffer. Maltose binding protein (pMYB5; New England Biolabs, USA) and unsubstituted agarose beads were used as negative controls.

c) UV-Vis absorption spectroscopy. All absorbance spectra were recorded in a quartz cuvette (Starna Pty Ltd. Australia) using a Beckman DU800 spectrophotometer (Beckman Coulter, USA). The absorption spectrum of monomeric heme on binding to HusA was recorded in 250 mM NaCl, 50 mM PIPES, pH 6.5. To further evaluate the bisheme binding property, holo-HusA was prepared by incubation apo-HusA with heme (ratio of 1:1) at 25°C for 20 mins in 250 mM NaCl, 100 mM Tris, pH 8.0. The HusA-heme complex was purified over a Sephadex G25 desalting column (1 cm × 10 cm) to remove free heme before the absorption spectrum of holo-HusA was recorded. Subsequently, sodium dithionite crystals (~1 mg) were added and the spectra under these reducing conditions were recorded. For kinetic absorption spectra, similar conditions as above were used with measurement carried out at pre-determined time points. All spectra were collected at 25°C. The observed rate constant was calculated using Prism software (GraphPad software Inc, California, USA).

d) Tryptophan fluorescence quenching assays. The binding affinity of rHusA to heme was investigated using the perturbation of intrinsic tryptophan fluorescence with a Luminescence spectrometer LS 50B (Perkin Elmer, USA) using a 10 mm path length quartz cuvette (Starna Pty Ltd. Australia). Fluorescence intensity at 338 nm with 295 nm excitation was recorded for 1000 µl of 400 nM rHusA in 100 mM Tris buffer, pH 8.0 and at 10 minutes after each subsequent titration of 0.5 µL of 80 µM fresh heme stock into the sample. The monomeric heme binding affinity assay was performed in 50 mM PIPES buffer, pH 6.5. The binding titration data were fitted to the equation below, in which a single binding site is assumed (15):

$$F_{obs} = F_0 + F_{max} \times \frac{[L]_t + [E]_t + K_d - \sqrt{([L]_t + [E]_t + K_d)^2 - 4[L]_t[E]_t}}{2[E]_t}$$

where F_{obs} is the observed fluorescence, F_0 is the initial fluorescence, F_{max} is the maximum amplitude of fluorescence quenching, $[L]_t$ is the total ligand concentration, $[E]_t$ is the total concentration of protein, and Kd is the apparent dissociation constant. The average Kd values from three independent assays were reported for each condition.

Size exclusion chromatography. Analytical gel filtration chromatography was carried out using a Superdex 75 10/300 GL column (GE Healthcare, USA) coupled to an ÄKTA™ purifier system with multiple wavelength sensor (GE Healthcare, USA).

The column was pre-equilibrated with 250 mM NaCl, 100 mM Tris, pH 8.0 at a flow rate of 0.8 ml/min prior to sample loading of 12.5 µM rHusA with/without 12.5 µM heme in a total volume of 400 µl. Protein elution was monitored at 280 nm and heme absorption at 399 nm and 385 nm. The column was calibrated with blue dextran 200 (void volume), conalbumin (75 kDa), carbonic anhydrase (29 kDa), ribonuclease A (13.7 kDa), and aprotinin (6.5 kDa) (GE Healthcare, Australia).

Cell fractionations and protein localization studies. Sub-cellular components were separated by Sarkosyl treatment and analytical centrifugation as previously described (16). Briefly, cultures were adjusted to OD_{600} of 0.5 with cold PBS buffer, pH 7.4 and treated with protease inhibitors: 4 mM *Nα*–tosyl–lysine chloromethyl ketone (TLCK) and 1% (v/v) protease inhibitor cocktail (Sigma-Aldrich, Australia) for ≥ 2 hours at 37°C. Bacteria were pelleted by centrifugation at 6,000 × *g* for 30 min and the supernatant was further ultracentrifuged at 150,000 × *g* for 1 hour to separate vesicles and vesicle-free media. Proteins in the supernatant fraction were precipitated by a pyrogallol red-molybdate-methanol (PRMM) method (17). Purity of the outer membrane fraction was confirmed by the exclusive presence of LPS and the purity of the inner membrane fraction by the exclusive presence of a biotin-containing oxaloacetate decarboxylase as detected by Western blotting using anti-LPS 1B5 mAb and alkaline-phosphatase AP-conjugated streptavidin, respectively (16).

Western blotting. Known amounts of protein antigen or whole bacterial cell cultures were standardized, separated by SDS-PAGE and electroblotted onto 0.2 *µ*m nitrocellulose membranes (Bio-Rad Inc., USA). Membranes were blocked with 2% bovine serum albumin in PBS buffer for ≥ 2 hours. Anti-HusA polyclonal antibody was produced through a subcontractor (Genscript Inc., NJ, USA) by immunizing rabbits with a synthetic peptide GGGKDKALPFAEKS present near the C-terminus of HusA. Purified polyclonal antibody against HusA was used to probe the membranes at 1:5,000 dilution in TBST buffer for 3 hours. Patient sera from a cohort that has been reported previously to be positive for *P. gingivalis* and has reactivity towards *P. gingivalis* proteins (18) were used at 1:40 dilution in the same conditions above. Alkaline phosphatase-conjugated (AP) goat anti-rabbit or goat anti-human IgG (Dako Corp., USA) antibodies were used at 1:10,000 dilution in TBST before final color development with AP Conjugate Substrate Kit (Bio-Rad Inc., USA). Densitometric analysis was performed from scanned images in a linear range using ImageJ from NIH Image (*http://rsb.info.nih.gov*).

Quantitative RT-PCR. Chemostat cultures were diluted to OD_{600} of 0.6 with medium and stabilized with RNAprotect Bacteria Reagent (Qiagen, Germany) before RNA was extracted with the RNAqueous Micro kit (Ambion, Australia). Reverse transcription was carried out on 2 µl of total RNA using the AffinityScript QPCR cDNA Synthesis Kit (Stratagene, Australia) in a volume of 10 µl as per the manufacturer's instructions. Quantitative PCR were carried out in 25 µl singleplex reactions using 5 µl of 1:5 dilution of the cDNA along with TaqMan probe/primers against *husA* and 5 µL of 1:200 dilution of cDNA for the calibrator gene *16S* (see primers and probes in Table S2) on a Stratagene Mx3005P Real-Time PCR System® using the Brilliant® II QPCR Master Mix (Stratagene, Australia). Normalization and calibration methods were the same as in our previous publication (16).

Construction of P. gingivalis *husA mutant strain.* Creation of the deletional inactivation *husA* mutant was carried out as described previously (16). Briefly, a 1.2 kb upstream fragment (primers: 2227frAEcoRF and 2227frASacR, with SacI and EcoRI sites) and a 1.3 kb downstream fragment (primers: 2227frBPstIF and 2227frBSphIR, with PstI and SphI sites) to the *husA* gene (Genbank accession no. PG2227) were amplified from chromosomal DNA of *P. gingivalis* W83 by PCR and inserted into pUC19. A 2.2 kb *ermF/ermAM* cassette (primers: ermSacF and ermPstIR, with PstI and SacI sites) was amplified from the plasmid pVA2198 (19) and inserted into the modified plasmid above to create pWD7. All primers used in this study are listed in Table S2. Plasmids were verified by DNA sequencing prior to being electroporated into *P. gingivalis* W83 for homologous recombination into the genome to create a deletion of the gene. The *husA*-positive control mutant was created the same way except that the *husA* gene itself was amplified (primers 2227frCEcoRIF and 2227frCSacIR) and inserted into the plasmid rather than the upstream fragment

to the *husA* gene to create pWDC7. Transformed cells were selected on erythromycin eTSB agar and resistant clones were further confirmed by PCR and Southern blot using the *ermF/ermAM* DIG-labeled probe (Roche, Australia).

Growth experiments. Fresh colonies of *P. gingivalis* wild-type W83, deletion mutant WD7 and control mutant WDC7 were inoculated into eTSB medium without heme supplementation as the starter cultures for growth curve analysis. Heme stores were depleted by daily passage of the starter culture into medium without heme supplementation at 1:10 inoculum until the biomass of the following passage could no longer attain an OD_{600} of 0.3 after 24 hours incubation. The penultimate culture was adjusted to OD_{600} of 0.5 and a 1:10 inoculum was transferred anaerobically into 5 ml of pre-warmed, pre-reduced eTSB medium supplemented with 50 nM or 5 μM heme in individual Teflon screw-cap test tubes (13 × 100 mm). Tubes were capped tightly, removed from the chamber and incubated at 37°C in a water bath. At pre-determined time points, tubes were vortexed and absorbance at 600 nm recorded using a Beckman DU640 spectrophotometer. Three independent experiments were performed in triplicate.

Statistical analysis. Prism v3.03 software (GraphPad Software Inc., USA) was used for all statistical analyses. Real-time PCR data and protein expression integrated densities from Western blotting were tested for normal distribution and differences were compared using one-way ANOVA, with Bonferroni's correction and 95% confidence intervals. Growth curve data from three independent experiments were expressed as mean and standard deviation and differences analysed by two-way ANOVA. *P* values of less than 0.05 were considered significant.

Results

HusA is a high affinity heme binding protein. To determine functional characteristics, purified and untagged recombinant HusA (rHusA) (Fig. S1) was incubated with heme, resolved on SDS-PAGE and initially stained with tetramethylbenzidine (TMBZ) to detect the presence of heme, followed by Coomassie Blue staining for protein detection. Heme was found to be associated with rHusA under reducing SDS-PAGE without boiling, but complete denaturation of the protein-heme complex by boiling of the sample resulted in the loss of staining for heme (Fig. 1A). This suggested that heme was strongly associated with rHusA but is not covalently bound to the polypeptide. The strength of heme-binding by rHusA was confirmed by its binding to hemin-agarose despite a wash step with 1 M NaCl and 0.5% Sarkosyl (Fig. S2).

Heme binding by rHusA was also detected by changes in the Soret region of the UV-visible spectrum of heme. Heme in solution exists as a monomer-dimer equilibrium (20). At pH 6.5, monomeric heme predominates giving an absorption peak at 365 nm (Fig. 1B). During incubation of HusA with monomeric heme, a shift in the Soret band peaking at 399 nm emerged which is accompanied by reduction in absorption at 365 nm. The emergence of μ-oxo heme was indicated by the shift of the charge transfer band (Q band) to 600 nm with reduction of the monomeric heme band at 630 nm (Fig. 1B inset) (12). This spectral pattern of heme absorption following ligation to HusA is also observed when heme monomer is incubated with gingipains which have been reported to mediate heme μ-oxo dimer formation in *P. gingivalis* (12).

To further evaluate the bisheme binding property of rHusA, rHusA-heme complex at pH 8.0 was purified by chromatography over a desalting column. Under these conditions, free heme demonstrated a doublet Soret band at 365 nm and 385 nm corresponding to monomeric and dimeric ferric heme respectively (Fig. 1C). This is in agreement with evidence that alkaline solutions favour the formation of dimeric species such as μ-oxo- or π-π^*-bisheme (20-21). Binding of heme to rHusA at pH 8.0 was associated with a shift in peak absorbance of dimeric heme from 385 nm to 399 nm with a slight shoulder at 375 nm. This was supported by an emergence of a charge transfer band at 600 nm (Fig. 1C), characteristic of a hemoprotein with ligated μ-oxo bisheme (12,22). Taken together, the spectrum indicated the primary binding mode of rHusA is to bisheme and the slight shoulder of the spectrum at 375 nm may indicate minor binding to other different heme species. Similar binding characteristics have been reported for the surface heme binding protein IsdH of *Staphylococcus aureus* (23). In order to investigate the nature of heme coordination by

HusA, the rHusA-heme complex was reduced with excess dithionite. Following reduction of Fe^{3+} to Fe^{2+}, the Soret band underwent a red shift with the appearance of two well resolved Q bands at 539 nm and 569 nm indicating the rapid formation of a low-spin ferrous heme (24-26) in the rHusA-heme complex (Fig. 1C). Binding of low-spin ferrous heme suggested HusA coordinates only to the fifth axis of the heme iron with the sixth coordination site being available for occupation by oxygen (27-28). This is analogous to binding by oxymyoglobin (29). Identical shifts in spectra were observed following incubation of rHusA with black pigment composed of μ-oxo dimers extracted from *P. gingivalis* (Fig. S3).

Kinetic interaction of rHusA with heme in solution at pH 8.0 was monitored by measuring time-dependent changes in the Soret absorption spectrum (Fig. 1D). Within 30 s of mixing into rHusA solution, there was a pronounced shift of the heme Soret band from 385 nm to 399 nm which progressively increased to reach equilibrium within 10 minutes. One phase exponential association curve fitting was employed to describe the kinetic behaviour of the absorbance signal. The observed rate constant K_{ob} was calculated to be $(4.3 \pm 0.4) \times 10^{-3}$ s^{-1} at 25°C. This indicated a fast association rate constant (k_{on}) for the kinetic interaction of heme with rHusA.

The heme-binding capacity of rHusA was determined by quenching of intrinsic tryptophan fluorescence (15). Sequential titration of 40 nM heme into 400 nM rHusA solution resulted in progressive quenching of rHusA fluorescence as shown in Figure 2. Control titrations were obtained using *N*-acetyltryptophanamide (NATA) as the fluorophore. Heme quenching data from the NATA solution were used to correct for inner filter effects of the titrant. The binding constant at equilibrium at pH 8.0 was calculated to be $7.0 \pm 2.5 \times 10^{-10}$ M, demonstrating high affinity binding of heme by rHusA. Moreover, binding saturation occurred at 400 nM heme titrated into 400 nM HusA, suggesting HusA bound heme at a stoichiometry of 1:1. Binding affinity of rHusA for monomeric heme at pH 6.5 was calculated as $1.0 \pm 2.2 \times 10^{-8}$ M, which was lower than for the dimeric form. The binding affinity for the extracted black pigment was $2.0 \pm 1.7 \times 10^{-9}$ M.

Dimerization of HusA by binding with heme. Recombinant apo-HusA is a stable monomer under experimental conditions used. However, the optical spectrum of HusA binding with heme indicated the presence of bisheme species. To probe the apparent anomaly of monomeric protein binding dimeric heme with 1:1 stoichiometry, molecular sieve chromatography was performed with UV-visible light spectroscopic analysis. As shown in Figure 3, in the absence of heme, rHusA migrated as a monomeric form with an apparent molecular mass of 21 kDa, estimated by the elution volume relative to that of molecular weight markers. In the presence of heme at a molar ratio of 1:1, a rHusA dimer peak in front of the monomer peak was observed in the chromatogram, associated with absorption at 399 nm and 385 nm used to monitor heme in the holo-HusA complex. The apparent molecular mass of the dimer complex was approximately 43 kDa (including the heme dimer of 1.233 kDa). This clearly illustrated the dependence of protein dimerization on the binding of heme. These data indicated that rHusA dimerized upon binding to bisheme. Similar observations also have been reported for heme binding proteins of the Gram-negative species *Pseudomonas aeruginosa* and *Campylobacter jejuni*, and the Gram-positive species *Streptococcal pyogenes* and *Staphylococcus aureus* (23,30-32).

Heme limitation up-regulates transcription and expression of husA. Expression of known heme uptake systems in *P. gingivalis* is often up-regulated in response to low levels of iron in the micro-environment (33). To investigate the role of heme concentration in the regulation of HusA expression, *husA* transcription and translation were studied in continuous cultures of *P. gingivalis* W83. Steady-state continuous culture is of value as mimicry of growth *in vivo* by enabling bacteria to be cultured under conditions of nutrient limitation. Continuous cultures of *P gingivalis* W83 at different heme concentrations were performed to probe *husA* transcriptional and translational responses by quantitative RT-PCR and Western blots, respectively. Transcription of *husA* was found to be inversely correlated to the concentration of heme supplementation with significant up-regulation in response to progressive reduction in heme from 2 μM to 0.05 μM (Fig. 4A). The level of *husA* transcription under 0.05 μM heme supplementation was approximately 3-fold higher than that under 0.1

μM heme and 20-fold higher than under heme replete conditions of 1 to 2 μM. Using Western blot with anti-HusA polyclonal antibody, expression of HusA in outer membrane fractions extracted from the same continuous cultures was found to correlate well to the level of *husA* transcription; highest production of HusA at 0.05 μM heme supplementation with minimal production under heme replete conditions (Fig. 4B, C). These findings indicated expression of *husA* was tightly controlled by environmental heme concentration.

HusA is critical for P. gingivalis growth under heme limitation. To examine whether the biochemical properties ascribed to HusA correlate with biological function, growth of wild-type *P. gingivalis* strain W83, *husA*-deleted mutant (WD7) and *husA*$^{+}$ control mutant (WDC7) were investigated under heme excess (5 μM) and heme limited (0.05 μM) conditions in batch culture (Fig. 5). In the absence of heme, none of the strains could grow after heme starvation (data not shown). Under a heme-limited environment of 0.05 μM heme supplementation, the WD7 strain did not grow whereas the wild-type and control mutant recovered (Fig. 5B). Under heme-replete conditions, all strains recovered from heme depletion (Fig. 5C). The data confirmed *husA* expression is essential for growth of *P. gingivalis* under heme-limited conditions.

HusA demonstrated hemophore-like function. The presence of an *N*-terminal signal peptide and absence of a membrane anchoring signal indicated HusA could be secreted. To test this, *P. gingivalis* W83 was grown under conditions of heme limitation and cellular fractionation was employed to separate proteins secreted into the medium from those tethered to the outer/inner membrane or located in periplasmic and cytoplasmic lysate. When analysed by Western blot using anti-HusA antibodies, HusA was found to be distributed on the outer membrane, secreted in extracellular vesicles and in the vesicle-free media fraction indicating that HusA could be secreted into extracellular milieu to function as a heme scavenger (Fig. 6A). A slightly higher level of HusA could be seen in the vesicle fraction. This observation is reminiscent of the hemophore HxuA of *H. influenzae*, which has also been reported to partition predominantly to the culture supernatant and outer membrane fractions (5,34). Thus, HusA is the first hemophore-like protein reported in *P. gingivalis*. Of note, the secreted form of HusA was readily detected in nutrient–rich enriched tryptic-soy broth (eTSB) medium supplemented with 0.05 μM heme but not in basal medium (BM) (35) with 0.05 μM heme (data not shown). The mechanism for different partitioning behaviour in differing media is unknown but it has precedence in the heme binding protein HtaA from the Gram-positive pathogen *Corynebacterium diphtheriae*. This protein is an iron-regulated heme binding protein which has been shown to be secreted during growth in nutrient-rich medium but is predominantly membrane-associated during growth in a semi-defined minimal medium (36). To further assess membrane-associated HusA, outer membrane fraction containing HusA was further separated by 2D-PAGE and immunoblotting. Six major isoforms in four clusters with isoelectric points ranging from 5.4 to 6.2 were detected on Western blot by anti-HusA antibody (Fig. 6B). Multiple isoforms of HusA may reflect the consequence of glycosylation or other posttranslational modifications to the expressed protein (37).

Humoral immune response to P. gingivalis HusA protein. To test whether HusA is expressed during infection by *P. gingivalis*, Western blot analysis of rHusA was performed against sera from periodontitis patients determined by PCR to be infected with *P. gingivalis*. All six sera from infected periodontitis patients reacted with rHusA. This result was interpreted to indicate that HusA was expressed during the course of infection and induced a specific immune response (Fig. 7).

Discussion

In human tissues, iron is sequestered by lactoferrin, transferrin and ferritin as a primary defence mechanism at the onset of infection (38). Microorganisms in turn, synthesise and secrete high affinity iron chelators, siderophores, to solubilise and take up Fe^{3+} (39). However, *P. gingivalis* does not produce siderophores or ferric reductases. Although *P. gingivalis* employs the Feo system to uptake ferrous iron in anaerobic or micro-aerophilic environments (40), growth studies have shown that *P. gingivalis* preferentially acquires iron in the form of heme, rather than from other sources (9,41). For *P.*

gingivalis, heme is also an essential nutrient source of protoporphyrin IX as the organism lacks the capacity to synthesize the porphyrin macrocycle *de novo* (2). To obtain exogenous heme and compete with other microorganisms, *P. gingivalis* expresses a number of outer membrane heme-binding proteins, particularly under heme-limiting growth conditions (42). However, no hemophore has previously been described for *P. gingivalis*.

Several heme binding envelope proteins, including OMP26, OMP32, HBP35, Tlr, HmuR, HmuY and IhtB, have been reported in cultured *P. gingivalis* (3,35,43-47). The majority of these are expressed under heme limited growth conditions where heme availability is less than 8.0×10^{-7} M (42,48). The best described heme uptake system in *P. gingivalis* is the *hmuYRSTUV* locus comprising two key components, HmuY and HmuR, both outer membrane proteins with relatively low heme binding affinity of 3.0×10^{-6} M and 2.4×10^{-7} M, respectively (3,49). Transcription of the *hmu* locus in *P. gingivalis* W83 strain is repressed by iron but induced by heme (3,46). No secreted extracellular heme-binding protein has been reported for *P. gingivalis* (33), although both high and low affinity heme receptors have been detected (50), with high affinity receptors induced in the presence of low heme concentrations (35).

HusA, as reported here, is a novel hemophore-like protein in *P. gingivalis*. A BLAST search revealed lack of significant homology between HusA and any known function proteins (*http://www.ncbi.nlm.nih.gov/blast*). Our findings showed that a significant proportion of total HusA protein synthesized by *P. gingivalis* under heme-limited conditions is released into the culture supernatant, as concluded from Western blot analysis of sub-cellular fractions (Fig. 6A). This finding has a precedent in the hemophore HxuA first reported as a lipoprotein on the surface of *H. influenzae* type b (Hib) and where some Hib strains secrete HxuA into the culture supernatant. Both forms of HxuA have been shown to scavenge heme from hemopexin (34,51). Unlike other hemophores, HusA has an unusual mode of heme binding as indicated by spectral absorption (Fig. 1), whereby iron from μ-oxo bisheme is presumably coordinated at the fifth position by HusA. Using size-exclusion chromatography and UV-Vis spectroscopy, we showed that apo-HusA is completely monomeric with dimerization occurring only following heme binding (Fig. 3). As fresh ferric heme exists predominantly as a dimer species in aqueous solutions at physiological pH, HusA binding to this entity may induce dimerization of the protein as observed. Interestingly, *S. marcescens* was reported to secrete a dimeric form of the hemophore HasA (DHasA) in response to iron deficiency conditions (14). DHasA with two heme molecules ligated at high affinity, serves the function of a heme reservoir in this organism (14). Compared with other heme binding proteins found in *P. gingivalis*, HusA was shown to have a much higher affinity at $7.0 \pm 2.5 \times 10^{-10}$ M for the cofactor (more than 1,000 times higher than HmuY with $K_d \sim 3 \times 10^{-6}$ M). Due to oxidation toxicity, in the host, free heme is rapidly sequestered by carrier proteins, including hemopexin, albumin and lipoproteins (52-53). With high heme binding affinity and fast heme association rate, HusA could be able to compete against certain host hemoproteins including serum albumin ($K_d \sim 1.0 \times 10^{-8}$ M) for free heme (49).

In *P. gingivalis*, genes encoding proteins involved in iron/heme transport are typically clustered together on the genome. Three multigenic clusters, the *iht*, *htr* and *hmu* loci, encoding proteins contributing to putative heme acquisition pathways, have been detected in the genome of *P. gingivalis* W83 (42). Deletion of the *husA* gene resulted in failure of growth under heme limitation (Fig. 5). Therefore, while the expression of multiple heme receptors including HmuY, Tlr and IhtB in response to heme limitation has been described for *P. gingivalis*, these heme uptake systems could not compensate for the deficiency of the *husA* deletion mutant under heme limitation. The open reading frame (ORF) located immediately upstream of *husA* encodes a hypothetical protein PG2226 identified as a heme-binding protein (unpublished data). We annotated this gene adjacent to *husA* as *husB* (see Fig. 5A). *husB* encodes an 83 kDa product with homology to TonB-dependent outer membrane receptors from other bacterial species, including an outer membrane siderophore receptor FpvA in *Pseudomonas aeruginosa*, sharing 33% similarity to HusB. Further, two additional ORFs are located directly upstream of *husB*. We designated these as *husC* (PG2225) and *husD* (PG2224). The *husD*

gene product is a hypothetical protein with little identity to other known functional proteins. BLAST analysis of *husC* predicted it to be a member of the MarR family of transcriptional regulators with significant identity (63%) and similarity (84%) to the MarR/emrR family of transcriptional regulators in *Prevotella* sp. Oral taxon 472. This homology extended to a number of additional MarR/emrR family transcriptional regulators and hypothetical proteins belonging to the order *Bacteroidales* including *Prevotella*, *Parabacteroides* and *Bacteroides species*. Proteins of the MarR family in bacteria have been reported to control a variety of biological functions, including oxidative potential and virulence (54). The MarR family transcriptional regulator PqrR of *Pseudomonas aeruginosa* was demonstrated to regulate expression of down-stream genes. Interestingly, the iron-containing prosthetic group in PqrR acts as a redox switch that regulates DNA binding activity and transcriptional repression (55). Recently, Lewis *et al.* reported that expression of *PG2227* (*husA)* and that of established heme uptake loci, was significantly down-regulated in the presence of oxygen (56). We also found that *husA* expression was significantly suppressed under high heme concentrations indicating the presence of a heme-sensing repressor of the *hus* locus. We propose a model in which HusC mediates repression of *husAB* under aerophilic conditions. Under these conditions, the presence of oxidized heme could accelerate the rate of HusC-heme assembly, increase DNA binding activity and reduce expression of the *husABC* locus. Alternatively, HusC may sense the presence of heme directly to negatively regulate expression of the *hus* locus. In either case, further investigation is needed to answer these questions.

In periodontally healthy individuals and during initiation of chronic periodontitis, *P. gingivalis* exists under conditions of heme limitation. The putative *hus* locus would be significantly up-regulated and augmented *husA* expression would be critical for successful establishment of *P. gingivalis* in subgingival plaque. Antibodies against HusA were detected in the sera of periodontitis patients with *P. gingivalis* infection, indicating HusA is expressed by *P. gingivalis in vivo*. Conservation of HusA function is indicated by alignment of HusA sequences from the annotated genomes of *P. gingivalis* strains W83 and ATCC33277 with 99% identity detected at DNA and protein levels.

In the host, hemoglobin is the major source of heme. Compared with other hemoproteins, hemoglobin is utilized more efficiently by *P. gingivalis* under heme-limiting conditions (41). The concentration of heme in healthy gingival fluid is low (57) and the ability to scavenge heme from limited hemoproteins, particularly hemoglobin, appears to be critical for the colonization of this organism *in vivo*. However, HusA cannot remove monomeric heme directly from hemoglobin or serum albumin (data not shown), a finding compatible with the observed preference of HusA for dimeric heme. *Porphyromonas gingivalis* has been reported to produce μ-oxo bisheme from hemoglobin through the action of a family of cysteine proteases, the gingipains. These comprise arginine-specific RgpA, RgpB and lysine-specific Kgp (58). RgpA has been reported to induce formation of methemoglobin containing Fe^{3+}, resulting in a decreased affinity of hemoglobin for the prosthetic heme molecule (59). This enhances degradation of hemoglobin by Kgp and the subsequent release of monomeric heme for capture by the hemagglutinin domains of this proteinase as μ-oxo bisheme (60). Bisheme formation has been confirmed to be promoted by the HA2 hemagglutinin domain within Kgp (12). Several heme receptors have been reported in *P. gingivalis*, however, none of these has been shown to act as a bisheme scavenger. Here, we showed that HusA has a preference for dimeric heme with high affinity and may serve as the predominant bisheme chelating protein under low heme growth conditions. Subsequently, holo-HusA is proposed to transport heme directly to a specific receptor, HusB, an integral outer membrane protein, for uptake by the organism. A schematic representation of this pathway is proposed in Figure 8. The model of a hemophore with a surface-attached recipient has precedence in other hemophore-dependent heme uptake systems. For instance, *S. marcescens* secretes HasA, a hemophore that transfers captured heme to a TonB-dependent outer membrane protein HasR (61). Clearly, further investigations are needed for a better understanding of the mechanism of heme uptake through HusA.

In conclusion, the findings reported here describe a novel hemophore-like protein, HusA, which essentially mediates growth of *P. gingivalis* under conditions of limited heme availability. To our knowledge, it is the first report of a high-affinity bisheme binding protein in *P. gingivalis*, which indicates unique structural and functional characteristics that may offer potential targets for future therapeutic intervention strategies.

REFERENCES

1. Wandersman, C., and Delepelaire, P. (2004) *Annu. Rev. Microbiol.* **58**, 611-647
2. Roper, J. M., Raux, E., Brindley, A. A., Schubert, H. L., Gharbia, S. E., Shah, H. N., and Warren, M. J. (2000) *J. Biol. Chem.* **275**, 40316-40323
3. Simpson, W., Olczak, T., and Genco, C. A. (2000) *J. Bacteriol.* **182**, 5737-5748
4. Arnoux, P., Haser, R., Izadi, N., Lecroisey, A., Delepierre, M., Wandersman, C., and Czjzek, M. (1999) *Nat. Struct. Biol.* **6**, 516-520
5. Hanson, M. S., Pelzel, S. E., Latimer, J., Muller-Eberhard, U., and Hansen, E. J. (1992) *Proc. Natl. Acad. Sci. U. S. A.* **89**, 1973-1977
6. Maresso, A. W., Garufi, G., and Schneewind, O. (2008) *PLoS. Pathog.* **4**, e1000132
7. Holt, S. C., Kesavalu, L., Walker, S., and Genco, C. A. (1999) *Periodontol. 2000.* **20**, 168-238
8. Gibson, F. C., 3rd, Ukai, T., and Genco, C. A. (2008) *Front. Biosci.* **13**, 2041-2059
9. Periasamy, S., and Kolenbrander, P. E. (2009) *J. Bacteriol.* **191**, 6804-6811
10. Fujise, O., Miura, M., Hamachi, T., and Maeda, K. (2006) *J. Periodontol.* **77**, 1333-1339
11. Bramanti, T. E., Holt, S. C., Ebersole, J. L., and Van Dyke, T. (1993) *J. Periodontal. Res.* **28**, 464-466
12. Smalley, J. W., Birss, A. J., Szmigielski, B., and Potempa, J. (2006) *Microbiology* **152**, 1839-1845
13. Smalley, J. W., Silver, J., Marsh, P. J., and Birss, A. J. (1998) *Biochem. J.* **331 (Pt 3)**, 681-685
14. Czjzek, M., Letoffe, S., Wandersman, C., Delepierre, M., Lecroisey, A., and Izadi-Pruneyre, N. (2007) *J. Mol. Biol.* **365**, 1176-1186
15. Shepherd, M., Heath, M. D., and Poole, R. K. (2007) *Biochemistry* **46**, 5030-5037
16. Nguyen, K. A., Zylicz, J., Szczesny, P., Sroka, A., Hunter, N., and Potempa, J. (2009) *Microbiology* **155**, 328-337
17. Caldwell, R. B., and Lattemann, C. T. (2004) *Appl. Environ. Microbiol.* **70**, 610-612
18. Nguyen, K. A., DeCarlo, A. A., Paramaesvaran, M., Collyer, C. A., Langley, D. B., and Hunter, N. (2004) *Infect. Immun.* **72**, 1374-1382
19. Fletcher, H. M., Schenkein, H. A., Morgan, R. M., Bailey, K. A., Berry, C. R., and Macrina, F. L. (1995) *Infect. Immun.* **63**, 1521-1528
20. Asher, C., de Villiers, K. A., and Egan, T. J. (2009) *Inorg. Chem.* **48**, 7994-8003
21. de Villiers, K. A., Kaschula, C. H., Egan, T. J., and Marques, H. M. (2007) *J. Biol. Inorg. Chem.* **12**, 101-117
22. Smalley, J. W., Birss, A. J., Withnall, R., and Silver, J. (2002) *Biochem. J.* **362**, 239-245
23. Watanabe, M., Tanaka, Y., Suenaga, A., Kuroda, M., Yao, M., Watanabe, N., Arisaka, F., Ohta, T., Tanaka, I., and Tsumoto, K. (2008) *J. Biol. Chem.* **283**, 28649-28659
24. Ghosh, K., Thompson, A. M., Goldbeck, R. A., Shi, X., Whitman, S., Oh, E., Zhiwu, Z., Vulpe, C., and Holman, T. R. (2005) *Biochemistry* **44**, 16729-16736
25. Vermeiren, C. L., Pluym, M., Mack, J., Heinrichs, D. E., and Stillman, M. J. (2006) *Biochemistry* **45**, 12867-12875
26. Wojtowicz, H., Wojaczynski, J., Olczak, M., Kroliczewski, J., Latos-Grazynski, L., and Olczak, T. (2009) *Biochem. Biophys. Res. Commun.* **383**, 178-182
27. Block, D. R., Lukat-Rodgers, G. S., Rodgers, K. R., Wilks, A., Bhakta, M. N., and Lansky, I. B. (2007) *Biochemistry* **46**, 14391-14402

28. Crosson, S., McGrath, P. T., Stephens, C., McAdams, H. H., and Shapiro, L. (2005) *Proc. Natl. Acad. Sci. U. S. A.* **102**, 8018-8023
29. Woodward, J. J., Martin, N. I., and Marletta, M. A. (2007) *Nat. Methods.* **4**, 43-45
30. Lansky, I. B., Lukat-Rodgers, G. S., Block, D., Rodgers, K. R., Ratliff, M., and Wilks, A. (2006) *J. Biol. Chem.* **281**, 13652-13662
31. Aranda, R. t., Worley, C. E., Liu, M., Bitto, E., Cates, M. S., Olson, J. S., Lei, B., and Phillips, G. N., Jr. (2007) *J. Mol. Biol.* **374**, 374-383
32. Chan, A. C., Lelj-Garolla, B., F, I. R., Pedersen, K. A., Mauk, A. G., and Murphy, M. E. (2006) *J. Mol. Biol.* **362**, 1108-1119
33. Olczak, T., Simpson, W., Liu, X., and Genco, C. A. (2005) *FEMS. Microbiol. Rev.* **29**, 119-144
34. Hanson, M. S., Slaughter, C., and Hansen, E. J. (1992) *Infect. Immun.* **60**, 2257-2266
35. Smalley, J. W., Birss, A. J., McKee, A. S., and Marsh, P. D. (1993) *J. Gen. Microbiol.* **139**, 2145-2150
36. Allen, C. E., and Schmitt, M. P. (2009) *J. Bacteriol.* **191**, 2638-2648
37. Troese, M. J., Sarkar, M., Galloway, N. L., Thomas, R. J., Kearns, S. A., Reneer, D. V., Yang, T., and Carlyon, J. A. (2009) *Infect. Immun.* **77**, 1746-1756
38. Sandy, M., and Butler, A. (2009) *Chem. Rev.* **109**, 4580-4595
39. Faraldo-Gomez, J. D., and Sansom, M. S. (2003) *Nat. Rev. Mol. Cell. Biol.* **4**, 105-116
40. Anaya-Bergman, C., He, J., Jones, K., Miyazaki, H., Yeudall, A., and Lewis, J. P. (2009) *Infect. Immun.*
41. Shizukuishi, S., Tazaki, K., Inoshita, E., Kataoka, K., Hanioka, T., and Amano, A. (1995) *FEMS. Microbiol. Lett.* **131**, 313-317
42. Lewis, J. P. *Periodontol. 2000.* **52**, 94-116
43. Bramanti, T. E., and Holt, S. C. (1992) *Microb. Pathog.* **13**, 61-73
44. Shibata, Y., Hiratsuka, K., Hayakawa, M., Shiroza, T., Takiguchi, H., Nagatsuka, Y., and Abiko, Y. (2003) *Biochem. Biophys. Res. Commun.* **300**, 351-356
45. Aduse-Opoku, J., Slaney, J. M., Rangarajan, M., Muir, J., Young, K. A., and Curtis, M. A. (1997) *J. Bacteriol.* **179**, 4778-4788
46. Lewis, J. P., Plata, K., Yu, F., Rosato, A., and Anaya, C. (2006) *Microbiology* **152**, 3367-3382
47. Dashper, S. G., Hendtlass, A., Slakeski, N., Jackson, C., Cross, K. J., Brownfield, L., Hamilton, R., Barr, I., and Reynolds, E. C. (2000) *J. Bacteriol.* **182**, 6456-6462
48. McKee, A. S., McDermid, A. S., Baskerville, A., Dowsett, A. B., Ellwood, D. C., and Marsh, P. D. (1986) *Infect. Immun.* **52**, 349-355
49. Wojtowicz, H., Guevara, T., Tallant, C., Olczak, M., Sroka, A., Potempa, J., Sola, M., Olczak, T., and Gomis-Ruth, F. X. (2009) *PLoS. Pathog.* **5**, e1000419
50. Tompkins, G. R., Wood, D. P., and Birchmeier, K. R. (1997) *J. Bacteriol.* **179**, 620-626
51. Cope, L. D., Thomas, S. E., Latimer, J. L., Slaughter, C. A., Muller-Eberhard, U., and Hansen, E. J. (1994) *Mol. Microbiol.* **13**, 863-873
52. Otto, B. R., Verweij-van Vught, A. M., and MacLaren, D. M. (1992) *Crit. Rev. Microbiol.* **18**, 217-233
53. Stojiljkovic, I., and Perkins-Balding, D. (2002) *DNA. Cell. Biol.* **21**, 281-295
54. Wilkinson, S. P., and Grove, A. (2006) *Curr. Issues. Mol. Biol.* **8**, 51-62
55. Rungrassamee, W., Ryan, K. C., Maroney, M. J., and Pomposiello, P. J. (2009) *J. Bacteriol.* **191**, 6709-6721

56. Lewis, J. P., Iyer, D., and Anaya-Bergman, C. (2009) *Microbiology* **155**, 3758-3774
57. Liu, X., Olczak, T., Guo, H. C., Dixon, D. W., and Genco, C. A. (2006) *Infect. Immun.* **74**, 1222-1232
58. Smalley, J. W., Birss, A. J., Szmigielski, B., and Potempa, J. (2008) *Biol. Chem.* **389**, 1235-1238
59. Smalley, J. W., Birss, A. J., Szmigielski, B., and Potempa, J. (2007) *Arch. Biochem. Biophys.* **465**, 44-49
60. Smalley, J. W., Thomas, M. F., Birss, A. J., Withnall, R., and Silver, J. (2004) *Biochem. J.* **379**, 833-840
61. Krieg, S., Huche, F., Diederichs, K., Izadi-Pruneyre, N., Lecroisey, A., Wandersman, C., Delepelaire, P., and Welte, W. (2009) *Proc. Natl. Acad. Sci. U. S. A.* **106**, 1045-1050

FOOTNOTES

* This study was supported by a grant LP0562660 from the Australian Research Council to NH and an establishment grant RN38/08 from the Ramaciotti Foundation to KAN. JG acknowledges the New South Wales Dental Board, Australia and Bela Schwartz Foundation, the University of Sydney, Australia for PhD scholarship support.

ACKNOWLEDGEMENTS

We thank Dr. Wei Zou, Ms. Nan Li for experimental assistance and discussions; Dr. Derek Harty for advice on chemostat cultures; Dr. Catherine Rathsam for advice on 2D-PAGE; Dr. Charles Collyer for advice on heme protein behaviour.

FIGURE LEGENDS

Fig. 1. Heme binding properties of HusA. **(A)** Pseudo-peroxidase activity of the rHusA-heme complex as detected by TMBZ staining of an SDS-PAGE gel. The same gel was re-stained with Coomassie Blue to show the apo-rHusA (lane 1), rHusA-heme complex boiled in reducing SDS-PAGE sample buffer (lane 2) and without boiling in reducing SDS-PAGE sample buffer (lane 3). **(B)** UV-Vis absorption spectra of heme incubated with recombinant HusA at pH 6.5. The Soret region for monomeric heme (365 nm) demonstrates a red shift with a broad Soret region developing during the incubation period. The inset shows the change in the Q bands. **(C)** Steady-state UV-Vis spectra of hemin, purified rHusA-heme complex and rHusA-heme complex with sodium dithionite at pH 8.0. The Soret region of heme shifted from Abs_{max} 385 nm to 399 nm on binding to rHusA. Following reduction of the ferric iron with the dithionite, the Abs_{max} of the Soret region shifted further to 416 nm with better resolved Q bands. Increased absorbance at 370 nm under reducing conditions was attributed to sodium dithionite. Inset is an enlargement of the far-visible spectrum to show the Q bands. **(D)** Time-resolved spectra showing increases in absorbance over time in the Soret region of the mixtures of rHusA and heme at stoichiometry ratio 1:1 at pH 8.0. Inset shows the increase in absorbance at 399 nm versus time. The change in absorption was modelled to a one phase exponential association equation to determine the K_{ob}.

Fig. 2. HusA binds heme with high affinity. Tryptophan fluorescence quenching data of sequential titration of 40 nM monomeric heme (pH 6.5) (▲), dimeric heme (pH 8.0) (◆) and pigment extracts (pH 9.8) (■) into 400 nM rHusA in 100 mM Tris buffer, pH 8.0. Control quenching titrations was obtained using 90 nM *N*-acetyltryptophanamide (NATA) (15) under the same conditions.

Fig. 3. HusA dimerization induced by heme at pH 8.0. Gel filtration chromatography showing rHusA-heme complex migrating as a protein dimer. Absorbance wavelengths were set at 280 nm for protein detection; heme absorption at 385 nm and rHusA-heme mixture at 399 nm, respectively. The molecular

weights were calculated using a calibration curve (inset) generated using the following standard proteins (GE Healthcare, USA): conalbumin (75 kDa), carbonic anhydrase (29 kDa), ribonuclease A (13.7 kDa) and aprotinin (6.5 kDa).

Fig. 4. Regulation of *husA* in response to environmental heme concentrations. **(A)** Relative transcription of *husA* mRNA in *P. gingivalis* cultured under various levels of heme supplementation were normalised against the housekeeping gene 16s rRNA. Results represent mean value of two independent experiments in triplicate ± s.e.m. **(B)** Similar analysis by immunoblot using anti-HusA polyclonal antibody to quantify the production of HusA in the outer membrane fraction. Bacterial cultures were adjusted to OD_{600} of 0.5 before outer membrane extraction as per Methods. **(C)** Densitometry of bands was measured as integrated density values (band area × relative intensity) to determine the quantity of expressed proteins using NIH image/ImageJ software. Data were calculated from two separate experiments. Significant differences from the heme replete condition of 2 μM were analysed by one-way ANOVA: **, $P<0.01$; ***, $P<0.001$.

Fig. 5. *P. gingivalis* requires *husA* for growth under heme-limited conditions. **(A)** The genomic maps of wild-type, *husA*-deletion mutant (WD7) and *husA*$^+$ control mutant (WDC7). The terminator stem-loop is indicated at the 3′ end of the *husA* gene in W83. **(B and C)** Growth of heme-depleted *P. gingivalis* wild-type W83 (●), *husA*-deletion mutant (○) and *husA*$^+$ control mutant (▼) in eTSB medium supplemented with 0.05 μM (B) and 5 μM (C) heme.

Fig. 6. Sub-cellular localization and detection of HusA isoforms. **(A)** Continuous culture of *P. gingivalis* grown under 0.05 μM heme supplementation was fractionated into equi-volume sub-cellular fractions in the presence of protease inhibitor cocktails as per Methods. Western blot using anti-HusA showing presence of the protein in extracellular fractions and extracts from the outer membrane of the organism. **(B)** Outer membrane fractions extracted from *P. gingivalis* W83 grown under heme-limited condition were separated on 2D-PAGE gel followed by immunoblotting with anti-HusA. A series of spots ranging from isoelectric points of 5.4 to 6.2 and at apparent molecular weight of 26 kDa, are recognized.

Fig. 7. Immunoreactivity of chronic periodontitis patients' sera with recombinant HusA by Western blot. Individual patient sera (numbered) were diluted 1:40 and hybridized to the blot as previously reported (18). The positive control band (lane +) was probed with rabbit polyclonal anti-HusA antibody as the primary antibody.

Fig. 8. Proposed model for heme transport via HusA in *P. gingivalis*. Under heme limitation, *P. gingivalis* up-regulates Kgp expression to degrade host methemoglobin and release monomeric heme. The hemagglutinin domains of Kgp convert heme monomer into heme μ-oxo dimer. Tethered HusA captures bisheme which is delivered to HusB, a predicted TonB-dependent integral outer membrane protein (OM), for transport of heme into the periplasm. In addition, *P .gingivalis* may also secrete soluble HusA to compete with other heme sequestering proteins and scavenge available free heme released from other organisms or dying cells.

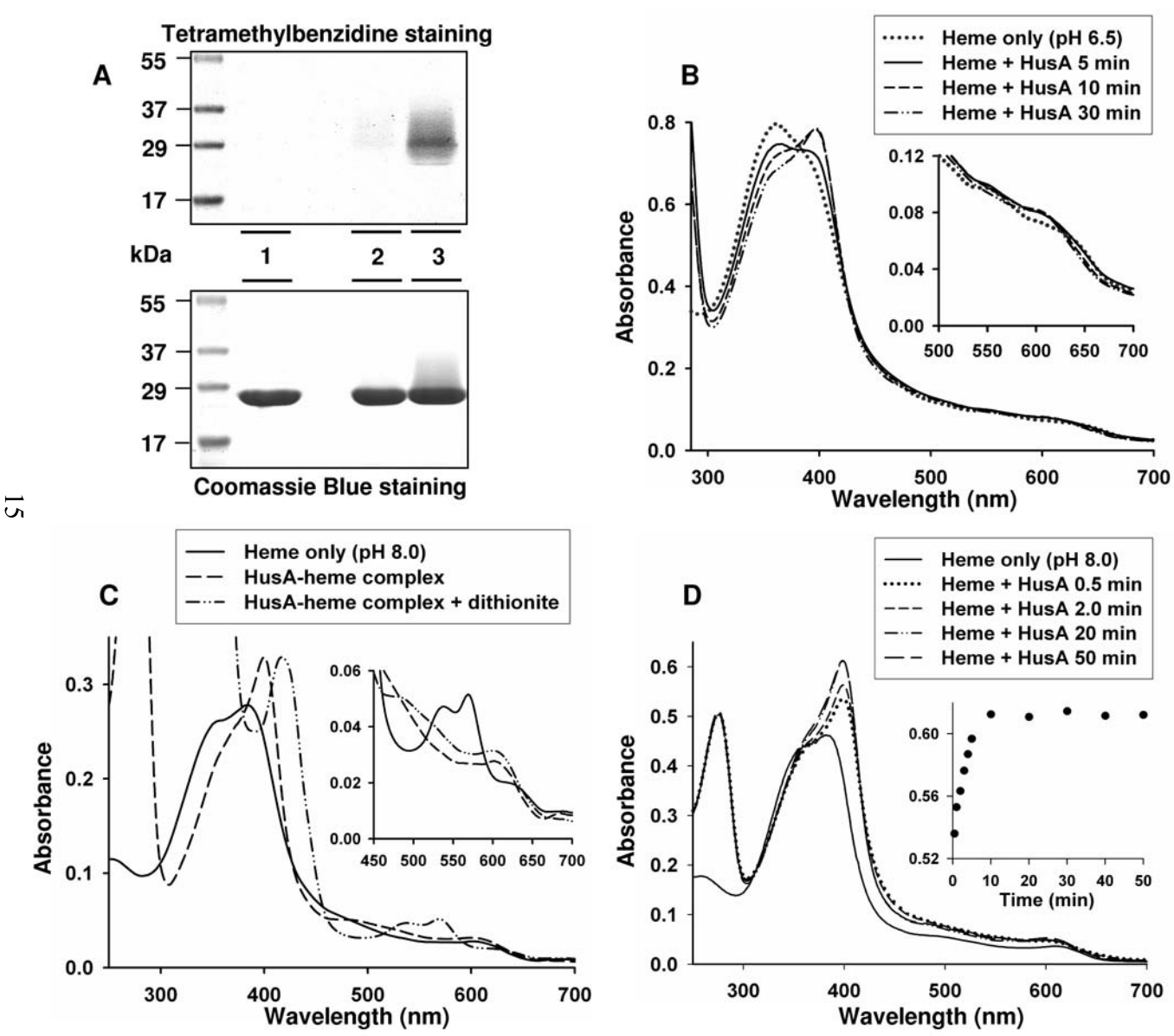
A
Tetramethylbenzidine staining
55
37
29
17
kDa
1
2
3
55
37
29
17
Coomassie Blue staining
B
Heme only (pH 6.5)
Heme + HusA 5 min
Heme + HusA 10 min
Heme + HusA 30 min
Absorbance
Wavelength (nm)
C
Heme only (pH 8.0)
HusA-heme complex
HusA-heme complex + dithionite
Absorbance
Wavelength (nm)
D
Heme only (pH 8.0)
Heme + HusA 0.5 min
Heme + HusA 2.0 min
Heme + HusA 20 min
Heme + HusA 50 min
Absorbance
Time (min)
Wavelength (nm)

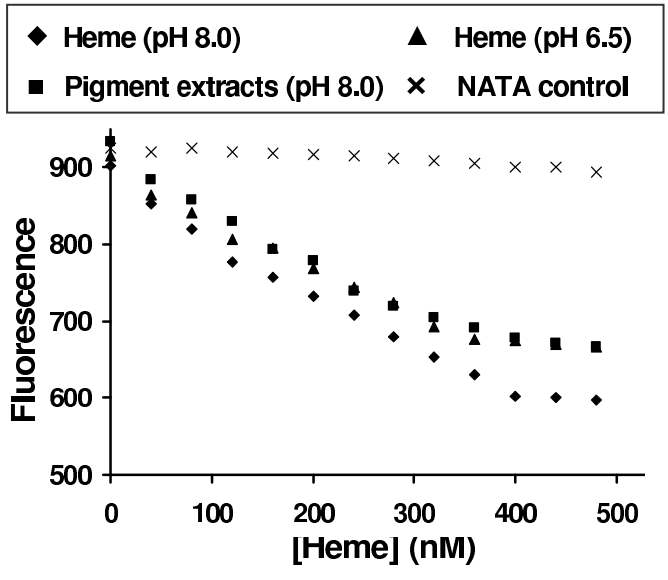
Heme (pH 8.0)
Heme (pH 6.5)
Pigment extracts (pH 8.0)
NATA control
Fluorescence
900
800
700
600
500
0
100
200
300
400
500
[Heme] (nM)

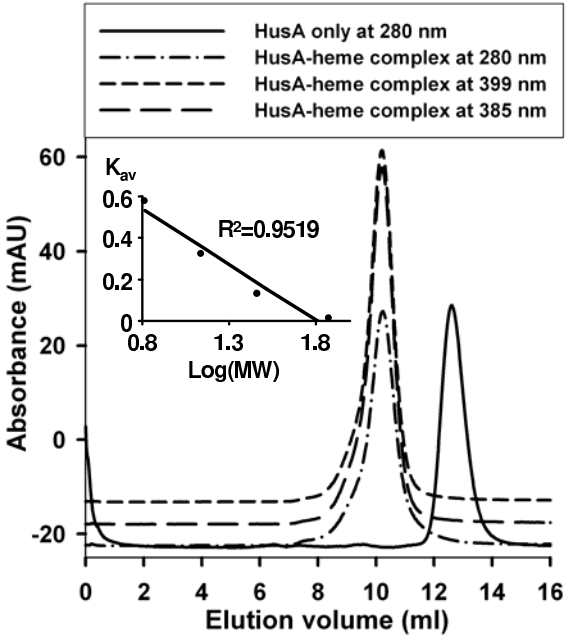
HusA only at 280 nm
HusA-heme complex at 280 nm
HusA-heme complex at 399 nm
HusA-heme complex at 385 nm
Absorbance (mAU)
Elution volume (ml)
K_av
R²=0.9519
Log(MW)

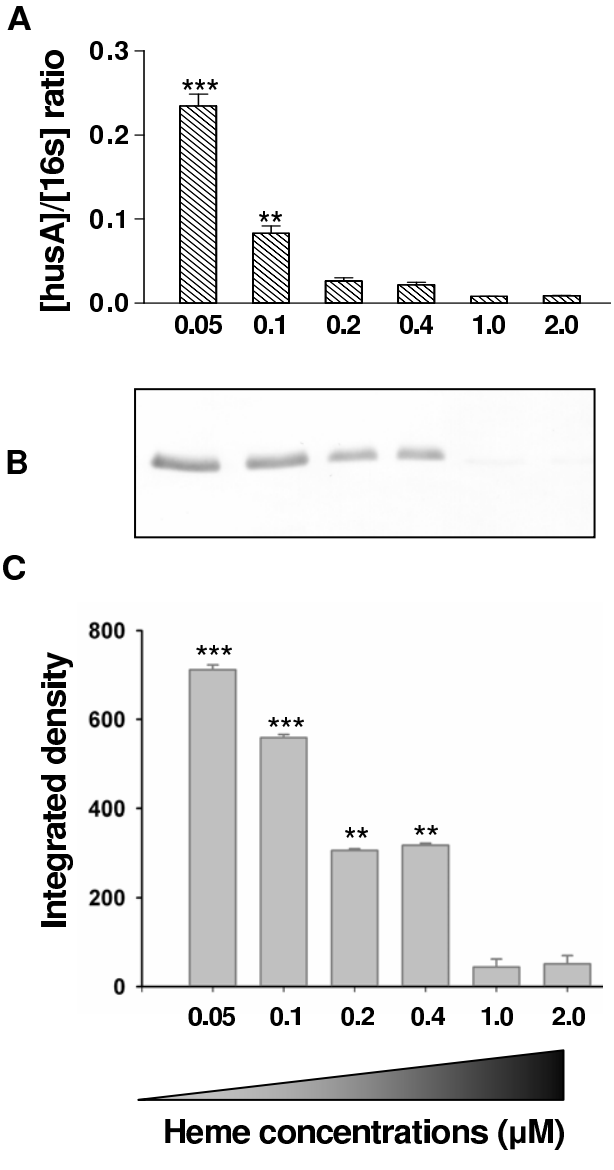
A
[husA]/[16s] ratio
0.3
0.2
0.1
0.0
***
**
0.05
0.1
0.2
0.4
1.0
2.0
B
C
Integrated density
800
600
400
200
0
***
***
**
**
0.05
0.1
0.2
0.4
1.0
2.0
Heme concentrations (μM)

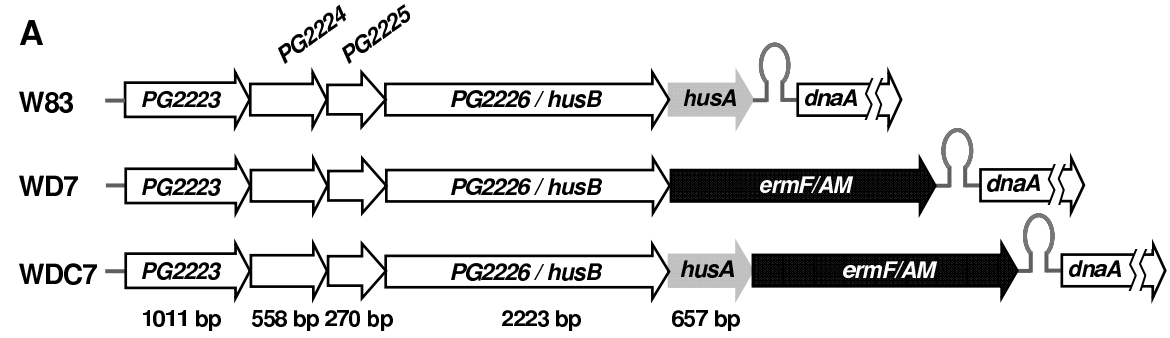
A
PG2224
PG2225
W83
PG2223
PG2226 / husB
husA
dnaA
WD7
PG2223
PG2226 / husB
ermF/AM
dnaA
WDC7
PG2223
PG2226 / husB
husA
ermF/AM
dnaA
1011 bp
558 bp
270 bp
2223 bp
657 bp

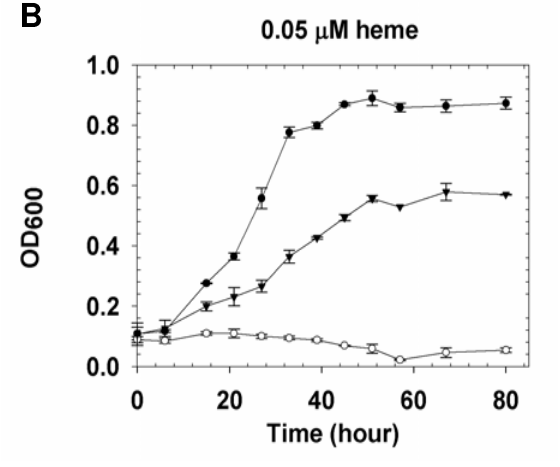
B
0.05 μM heme
OD600
Time (hour)
0.0
0.2
0.4
0.6
0.8
1.0
0
20
40
60
80

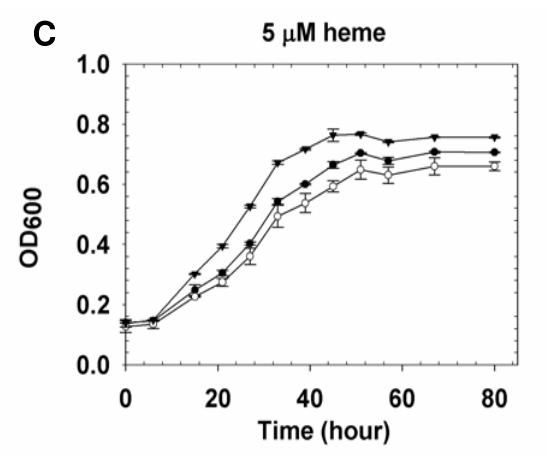
C
5 μM heme
OD600
Time (hour)
0.0
0.2
0.4
0.6
0.8
1.0
0
20
40
60
80

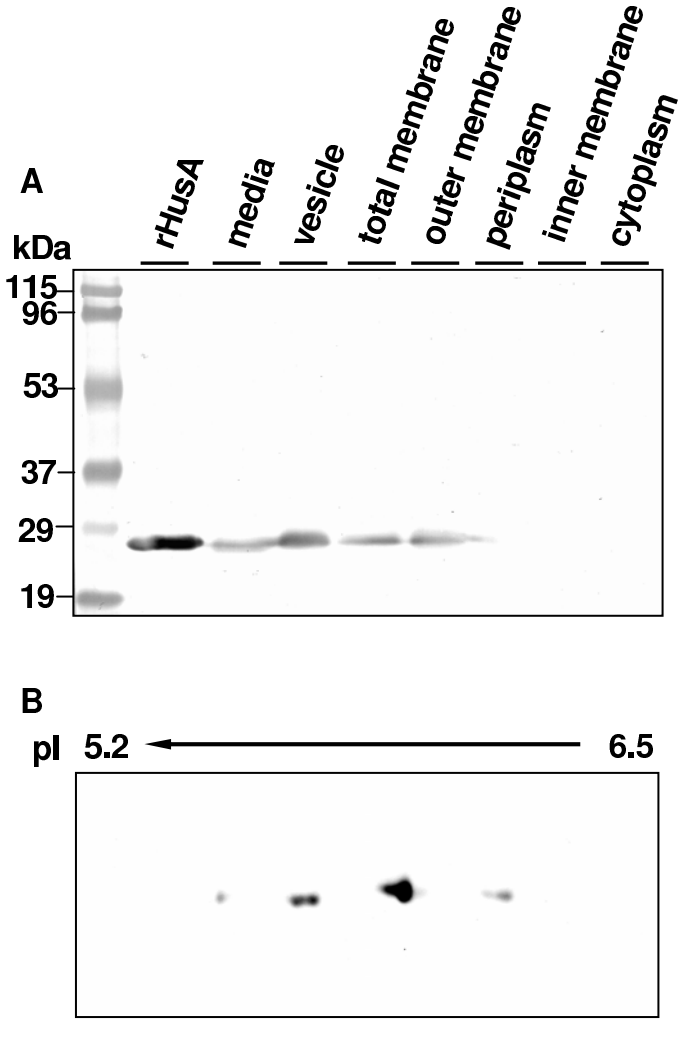
A
kDa
rHusA
media
vesicle
total membrane
outer membrane
periplasm
inner membrane
cytoplasm
115
96
53
37
29
19
B
pI
5.2
6.5

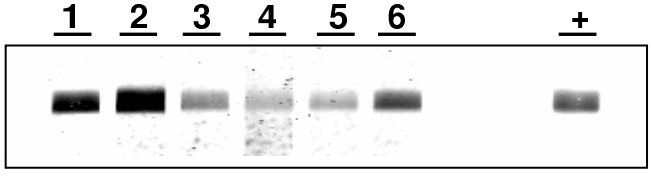
1
2
3
4
5
6
+

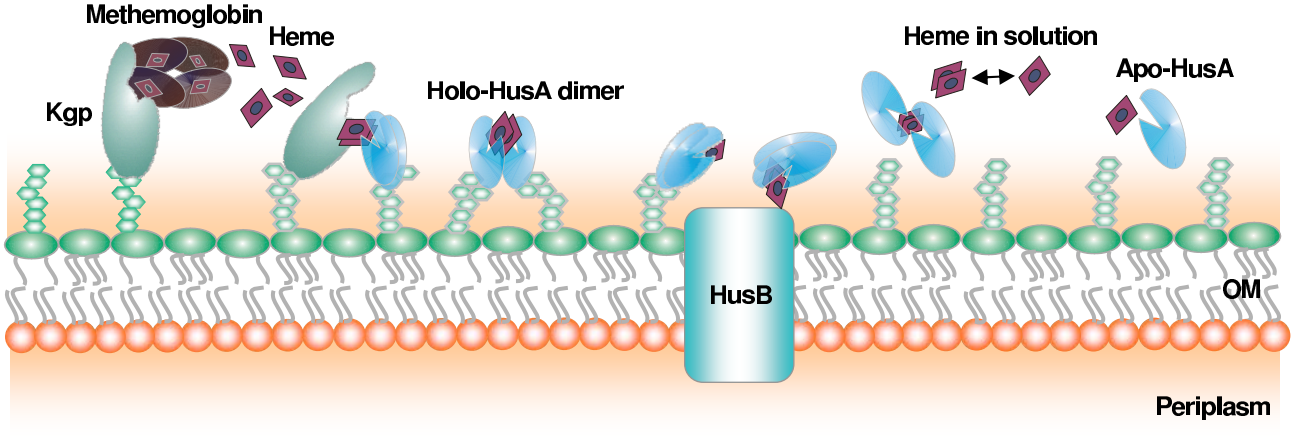
Methemoglobin
Heme
Kgp
Holo-HusA dimer
Heme in solution
Apo-HusA
HusB
OM
Periplasm